RESEARCH ARTICLE OPEN ACCESS

Characterization of New Cast Iron Alloys for the Stub-Anode Connection in the Aluminium Reduction Cells

Adel Nofal[1], Mohamed M. Ali[2], Amr Kandil[3] and Mahmoud Agour[4]
[1] Central Metallurgical R&D Institute (CMRDI), P.O. Box 87 Helwan, Egypt
[2]Al Azhar University, Faculty of Engineering, Qena, Egypt
[3]Al Azhar University, Faculty of Engineering, Cairo, Egypt
[4]Aluminum Co. of Egypt (Egyptalum), Nagaa Hammadi, Egypt

Abstract
High phosphorus gray iron (HPGI) is used to connect the steel stub of an anode rod to a prebaked anode carbon block in the aluminium reduction cells. The electrical resistance and resistivity properties, for different grades of cast iron, were tested and measured at different temperatures - using bench scale set ups- and evaluated as a potential replacement for the existing HPGI due to the limitations of that material. These cast iron alloys include low-phosphorus gray iron, ductile irons with compositions typical for ferritic (FDI), pearlitic (PDI) ductile iron grades and three alloys with low phosphorous irons with different carbon equivalents. The thermal expansion for steel stub, HPGI, and for the succeeded cast iron alloy was measured using high precision automatic dilatometer and analyzed. Microstructures and mechanical properties of the selected alloy were tested and compared with the existing HPGI.
The results shown that, the contact pressure, at steel stub-cast iron collar-anode connection, plays the major role in determining the electrical resistance and hence the voltage drop. Gray iron with carbon equivalent=4.5 has the lowest electrical resistivities compared with the other tested cast iron alloys, meanwhile carbides in the as-cast structures seem to be beneficial in increasing the thermal expansion and hence the contact pressure during the anode service life. The saving percent in voltage drop between gray iron with carbon equivalent =4.5 and HPGI reached to 18%.
Keywords- Different cast iron alloys, microstructure, electrical resistivity and resistance, thermal expansion and mechanical testing

I. Introduction

In the early days of aluminium electrolysis a direct contact between the iron stub and prebaked anode block was used. The conical iron stub had a sharp-edged conical thread and was screwed into a slightly tapered stub hole of the prebaked anode block. Other types of stub-anode connections are known where the electrically conductive bridge between iron stub and prebaked block was made by ramming or gluing pastes the presently applied stub-anode connection of prebaked anodes. The contact between iron stub and prebaked anode block was made by cast iron which has good thermal expansion, electrical resistivity and thermal conductivity [1].

Currently cast iron is used to provide good electrical, mechanical and thermal contact between anode carbon block and steel stub [2-5]. Cast iron considered the material of choice more for its excellent founding characteristics than its electrical conductivity. The composition of cast iron has been designed to ensure high fluidity in order to fill the cavity between the steel stub and anode carbon block; this is achieved at the expense of the electrical conductivity of the iron, which is decreased by phosphorus, silicon and carbon. Manganese and sulfur react to form MnS, forming inclusions that further affect the electrical characteristics of the rodding process. Phosphorus has been believed to enhance contact between cast iron collars and anode carbon leading to lower stub-anode voltage drop. Moreover, phosphorous has been shown to increase the electrical resistively and reduce the thermal conductivity of cast iron significantly [6-11]. Angus [10] confirmed that up to 0.2% phosphorus has an almost negligible upon electrical resistivity, but above 0.2 % the phosphorus an effect on the graphite structure which produces an increase in resistivity.

Electrical power accounts for the largest part of the aluminum production cost, it is believed that there is much works to improve the power efficiency of this complex process by optimizing electrode design and procedure, reducing the stub-anode voltage drop or optimizing the design of the steel stub hole for minimum voltage drop [1-4, 12, 13]. Moreover, it has been recently demonstrated, that it is not the contact surface but the contact pressure, what determines the voltage drop at the cast iron anode interface. So the voltage drop across the stub-anode interface is usually taken as a measure for the collar performance [6]. The casting process and the cast material give some challenges that need to minimize the energy loss in the finished stub-anode coupling.

These challenges include i) correct positioning of the stub in or close to the centre of the hole to ensure adequate filling of iron all the way around the stub, ii) control of the pouring rate of the cast iron, iii) control of the cast iron pouring temperature, and iv) control of the cast iron cooling rate[14].

Results of measurements of the electrical resistivity, thermal conductivity and thermal expansion as a function of temperature for three constitutive materials were studied, and the main conclusion is that the average voltage drop over approximately 90% of the anode cycle time is about 12 mV between stub and cast iron and about 120 mV between stub and carbon anode [1].

The performance of HPGI collars in the course of service cycle of an operational cell was studied by measuring the voltage drop between the stub-anode block connection and also the collar temperature measurement. The variation in the voltage drop was correlated to the changes in HPGI microstructure over a complete life cycle of the anode i.e. up to 30 days and at increasing temperatures up to 850°C. The electrical resistivity, resistance and thermal expansion for HPGI samples were tested and evaluated [15, 16].

This work was carried out to explore the potentials of testing six alternative cast iron alloys for stub-anode connection and comparing with the existing HPGI collar. The performance of these alloys was evaluated by measuring the electrical resistivity, electrical resistance of the collar connections, microstructure, mechanical testing ***and*** thermal expansion to simulate the dimensional behavior of different cast irons alloys at the operating temperatures of the electrolytic cells.

II. Experimental Work

Egyptalum has a big rodding plant started production in 1997. Each prebaked anode carbon block is connected to steel stub by pouring molten cast iron in specially designed holes in the carbon anode "the stub holes" to fill the gap between the steel stub and the anode. The cast iron ring formed is usually referred to as cast iron “collars". The solidified collars in the stub hole play the role of mechanical, thermal as well as electrical connection.

1- The chemical composition for the different cast iron alloys

Egyptalum smelter is used HPGI, which is poured in the gap between the steel stub and the anode carbon block. Quantity of HPGI used for each anode block is reached to 25 kg. The chemical analysis for the different cast iron alloys tested in this work is analyzed by ARL 3460 simultaneous quantometer.

2- Electrical resistivity and resistance measurements

To simulate the operating conditions in the steel stub/ collar/carbon anode connection, bench-scale experimental set-up [16] was designed and used for electrical resistance measurement. Carbon blocks 150 x 150 x 150 mm were cutted from the same anode carbon material used in the aluminum cell, and a stub hole 70 mm diameter was machined in the centre of the carbon block. Steel bars 60 mm diameter and 120 mm long were machined from Steel37 used to hang anodes in the actual electrolytic cells and fixed in the centre of the stub hole. The investigated alloys were poured in the gaps between the cylindrical steel bars and carbon blocks. Five blocks were worked for each alloy. Four blocks from them were placed in a resistance muffle furnace and gradually heated. These blocks were withdrawn from the furnace at some selected temperature. Individual blocks were held for two hours at each temperature before being taken out of the furnace for cooling.
Y-blocks from each of the investigated alloys were used to machine cylindrical rods 15 mm diameter x 200 mm length, which were used to measure the resistivity of the different cast iron alloys using the set-up [16].

3- Thermal expansion measurement

The behaviour of the stub material (Steel37) as well as the samples taken from the different cast iron alloys with 3 mm diameter x 10 mm length using a fully automatic dilatometer was tested and evaluated.

4- Hardness and tensile measurements

Brinell hardness was measured on the polished surfaces of the as cast collars using Wolpert Dia-testor 3b. Five readings were taken for each collars and the average hardness was determined. While the tensile testing of cast collars was measured according to EN 10002-1 using SCHENCK UTS 114-50. The test involves straining a test piece in tension, generally to fracture.

5- Collars microstructure for the selected cast iron alloys

Samples for the as cast collars were machined and polished for microstructure investigation. The model of optical microscope used in this work is Gold MCX1700.

III. Results and Discussion

1- The chemical analysis for the different cast iron alloys

Different cast iron alloys were analyzed and evaluated as potential replacement for the existing HPGI. Cast irons are iron-carbon-silicon alloys that always contain minor constituents (<0.1 %) and often alloying (>0.1 %) elements. The carbon content is normally in the range 3 to 4 % and the silicon content in the range 1 to 3%. The chemical composition for the selected alloys is listed in Table 1 and compared with HPGI. Typical chemical composition used for ferritic and pearlitic ductile irons production. The

results show that the FDI is lower in Mn and higher in Si contents and vice-versa in the PDI with 0.71% Cu. In this table, the last three cast iron alloys were poured from gray irons with different carbon equivalent; 3.9(hypoeutectic alloy), 4.3(the alloy is a eutectic) and 4.5 (hypereutectic alloy). Irons of the same CE value may be obtained with different carbon and silicon values. Manganese and sulfur are present in small amounts as residual impurities in all previous alloys except HPGI.

TABLE 1- CHEMICAL COMPOSITION FOR THE TESTED ALLOYS

Element, % / Type	C	Si	Mn	P	S/ Cu
High-P gray iron (HPGI)	**3.50**	**2.60**	**0.62**	**0.71**	**0.09**
Low-P gray iron(LPGI)	3.50	2.52	0.66	0.03	0.02
Ferrite ductile iron (FDI)	3.58	2.59	0.11	0.04	0.01
Pearlitic ductile iron (PDI)	3.63	2.16	0.36	0.02	0.01/ 0.71
Gray iron with CE=3.9	3.45	1.48	0.89	0.04	0.02
Gray iron with CE=4.3	3.52	2.05	0.90	0.04	0.02
Gray iron with CE=4.5	**3.53**	**2.68**	**0.88**	**0.04**	**0.02**

2- Analysis the electrical resistivity and resistance measurements

The resistivity of the investigated cast iron samples as well as the steel sample increases steadily with temperature as shown in Figure 1. Steel sample had the lowest electrical resistivity, and the difference between steel and cast iron resistivities decreases with increasing temperature. The electrical resistivity of steel increases almost by a factor of 10 between room temperature and 800°C[18]. When the temperature approaches the eutectoid at ferrite-austenite transition temperature, the resistivity values tend to level due to the higher density of ferrite iron.

The highest resistivity was illustrated for irons with the highest CE, and vice- versa for the irons with the lowest CE. This may be due to the higher amounts of graphite in the structure of irons with higher CE-values. The resistivities of LPGI and HPGI with flake graphite are higher than FDI & PDI with spheroidal graphite, where the resistivities of FDI slightly lower. As electrical conductivity is reduced with coarser graphite flake size, this may explain the resistivity of the LPGI is higher as compared with HPGI. Harmful effect of graphite flake size has masked that of the increased P-content as discussed in elsewhere [11, 19].

The electrical resistance at the collar connection is illustrated in Figure 2. The resistance of connections at 500°C using spheroidal graphite iron collars seems to be slightly higher than those using gray iron collars. This may be related to the higher as-cast shrinkage of irons with spheroidal graphite [18, 19]. However, with increasing temperature, the resistance of spheroidal graphite irons drops at a higher rate. The resistance of the connection at 800°C using the PDI collar falls most steeply and reaches to the lowest value. The contact pressure at the stub-collar-anode connection is largely affected on the electrical resistance. This is largely depended on the solidification expansion resulting from the precipitation of graphite during the eutectic reaction of iron with higher CE [16, 18].

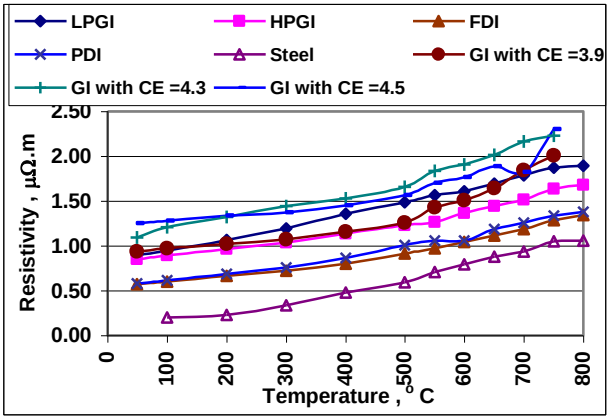

Figure 1- Electrical resistivity of different types of cast iron alloys as compared with steel sample.

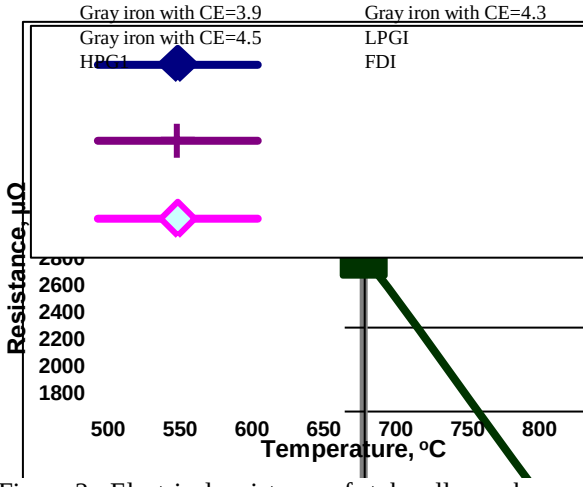

Figure 2 - Electrical resistance of stub collar-carbon block connection for the tested cast iron alloys.

After pouring the cast iron into the stub hole then left it to cool to the solidification temperature, an air gap between the collar and the anode block is happened due to the collar shrinkage. The shrinkage increases with the precipitation of primary austenite. The collars may suffer from further shrinkage as the eutectic solidification is started if they solidify according to the metastable system ($L \rightarrow \gamma$ + carbides) typical of low CE irons, or relative expansion if they solidify with the stable system ($L \rightarrow \gamma$ + graphite) typical of higher CE irons. More shrinkage takes place until the eutectoid temperature with continuous cooling in the solid-state, where relative expansion occurs due to the transformation of denser austenite to ferrite or pearlite.

Two important observations are obtained, the contact pressures leading to increase the electrical resistance at the stub-collar-anode connection and increase the expansion of cast iron after heating to 800°C, results in better contact and decrease the electrical resistance [18].

- Comparing results of Figures 1 and 2, and for example, the resistivity of FDI at higher temperatures is slightly lower than that of PDI, whereas the resistances of connections using PDI collars are significantly lower at the same temperature. This indicates that other factors, rather than the electrical resistivity of the collar contribute to determine the resistance of the stub-collar-anode connection.

It is clear from temperature measurements on the stub-collar-anode during anode life cycle (28-31 days) that the greatest period in the anode life (more than three weeks) is between 700-800oC[16], so that the comparison between the seven cast iron alloys with the electrical resistance were done at these temperatures as shown in Figure 3. The improvement percent in voltage drop between the existing HPGI and gray iron with CE=4.5 is 18.4 % as compared with 17.2 % with PDI.

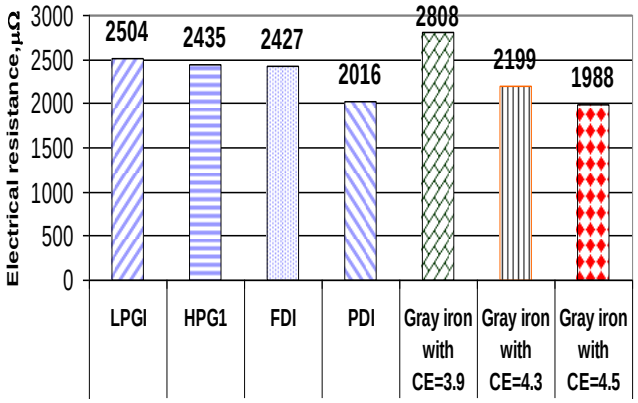

Figure 3- Average electrical resistance of stub anode connection at temperature from 700 -800 oC.

3. Thermal expansion measurement

Results from the dilatation measurements for the stub material as well as the selected cast iron samples are shown in Figure 4.

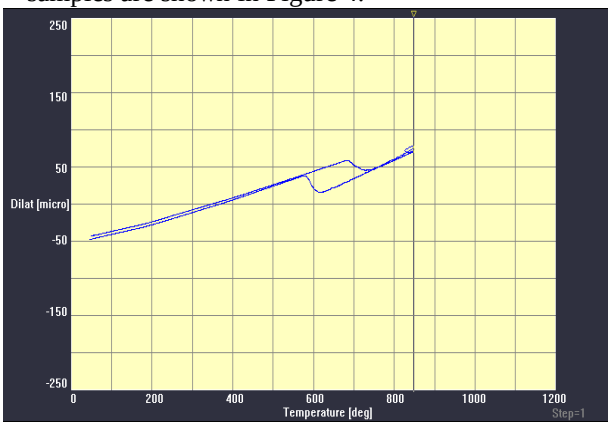

(a)

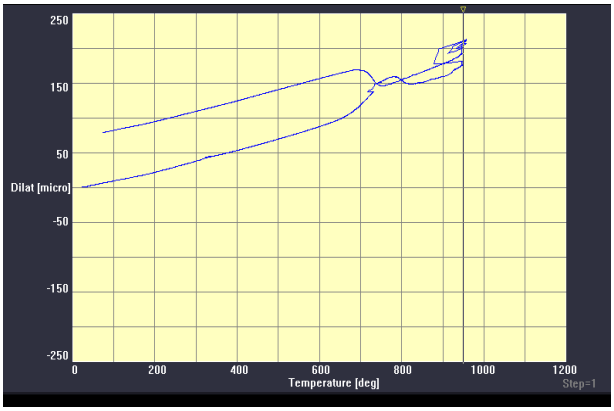

(b)

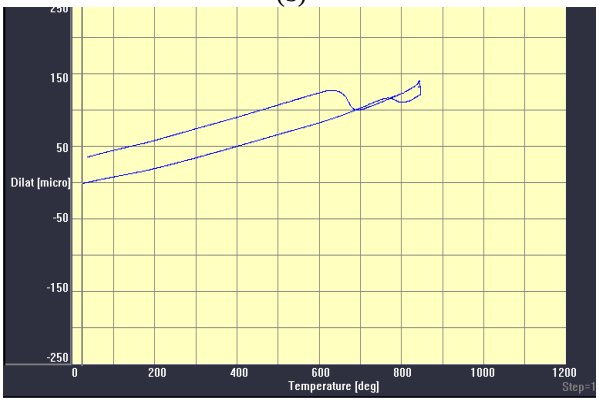

(c)

Figure 4- Thermal expansion curves of a) Steel, b) HPGI, c) Cast iron with CE=4.5.

When the volume of the various components increases, the electrical contact between them becomes more diacritics; this decreases the energy loss in these areas [20]. Typical contraction and expansion on heating and cooling is illustrated for steel associated with the eutectoid reaction and the formation of the more closed-packed austenitic structure on heating. Steel exhibits very slight dimensional change after the completion of the heating cooling cycle. Considerable permanent expansion after the completion of the heating-cooling cycle is shown for HPGI. The thermal expansion for CE alloy illustrates that iron with highest CE showed low extensive expansion due to graphitization of the ledeburitic matrix. The expansion decreases with increased CE containing lower amounts of carbides. The expansion values for the tested cast iron alloys may explain the electrical resistance data indicated in Figure 2, where more expansion of irons has a large affect in contact pressure and, hence, lower electrical resistance at the stub-collar-anode connections then affect cell performance [14, 16].

4- Hardness and tensile stress testing

The mechanical properties for the selected alloy is shown in Table 2 and compared with the currently used HPGI. No variations in hardness for gray iron with the nearly carbon content, graphite size and distribution

TABLE 2- MECHANICAL PROPERTIES FOR THE SELECTED CAST IRON ALLOY AS COMPARED WITH HPGI

Type of specimen	**Hardness, Brinell**	**Yield strength, N/mm^2**	**Ultimate tensile stress , N/mm^2**	
Gray iron with CE=4.5	180	60.7	1%	99
HPGI	180	82.3	1%	112

Elongation of gray iron with CE=4.5 at fracture is very small (of the order of 0.73%) as compared with 0.56 % for HPGI. And these values are nearly similar with the published data for gray iron at fracture (of the order of 0.6%).The stress-strain curve for gray iron with CE=4.5 is shown in Fig. 5. Gray iron does not obey Hooke's law, and the modulus in tension is usually determined arbitrarily as the slope of the line connecting the origin of the stress-strain curve with the point corresponding to one-fourth the tensile strength [21].

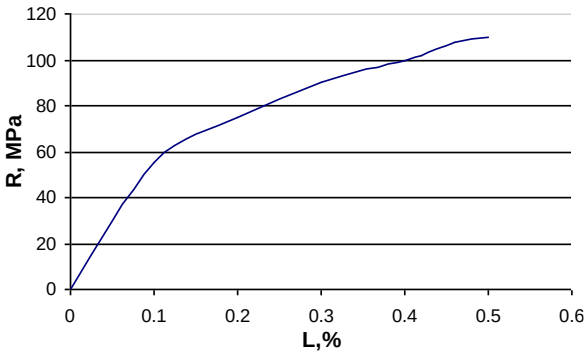

Figure 5- The stress-strain curve for gray iron with CE=4.5

5. Collars microstructure

The casted microstructure of HPGI shown in Figure 6 consists of pearlitic (P) matrix with fine undercooled graphite (UG) type-D flake graphite (interdendritic segregation, random orientation) may be formed near rapidly cooled surfaces. Frequently, such graphite is surrounded by a ferrite matrix (F) [21].

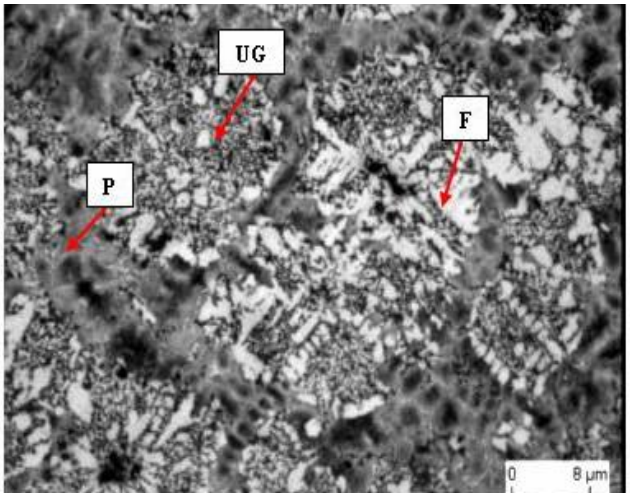

Figure 6- The as-cast microstructure of HPGI(0.5nital)

[

- The microstructure of gray iron with CE=4.5 consists of undercooled graphite (UG) in ferritic matrix(F), encircled with a network of pearlitic layer(P) at the grain boundaries of the sample (Figure 7)[17,19].

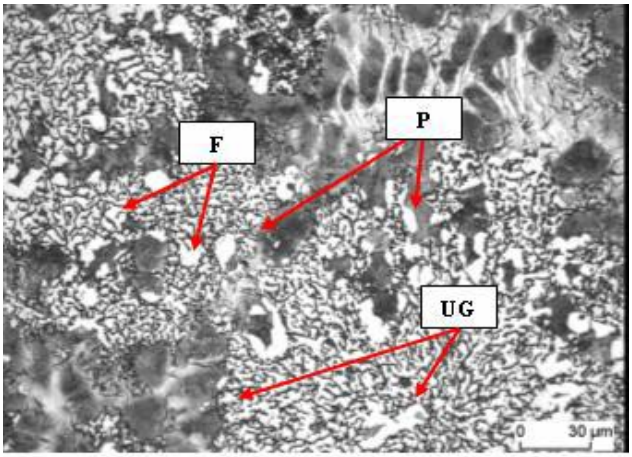

Figure 7- Microstructure of gray iron with CE=4.5

- Evaluation the performance of the selected alloy

Energy saving and consequence increase the aluminium productivity can be obtained from reducing the resistance of the current path in the aluminium reduction cells.

50 prebaked anodes were tested at Egyptalum cells after rodded in its rodding plant using gray cast iron with CE=4.5. The voltage drop can be reduced by 23mV, but for safe operation, the cell voltage was decreased by 10 mV. These rodded anodes were tested in one cell for 2 months without any change in cell behaviour or problems in the cast alloy.

A simple economic equation is used to calculate the money saving in one year if the cell voltage reduce by 1 mV in case of plant has 552 pots operating at 210 kA, assuming the energy cost is 0.3 Egyptian pound/kWh(1 dollar equals 6.8 E. pound).

$$1 \times 552 \times 210 \times 24 \times 365 \times 0.3 = 304638 \frac{E.pound}{year}$$

IV. Conclusions

Six cast iron alloys were prepared and tested experimentally to use some of these alloys as a replacement of the currently used HPGI.

Two bench- scale experimental set-ups have been used to simulate the operating conditions in the steel stub/ collar alloys/ anode block connection and used to measure the electrical resistance and resistivity respectively.

Gray iron with CE=4.5 may represent a favorable material for the stub-anode connection collars instead of HPGI, where the electrical resistivity reduces, and voltage drop improves. The gray iron with CE=4.5 can be tested on whole potline with reducing the cell voltage by 23 mV on two steps during six months with carefully attention to other operation procedures.

V. ACKNOWLEDGMENT

The Authors would like to express their appreciation to Chairman and executive director of Egyptalum for his support during this work. The great thanks to the contributions of heads of the production sectors, carbon and refractories sectors, technical sectors and head of R & D sector of Egyptalum for saving the best conditions to success this work. Also, the authors would like to thank the teams of Central Metallurgical R&D Institute (CMRDI), R & D and laboratories managements of Egyptalum for their continuous helping during this work.

REFERENCES

[1] S. Wilkening & J. Côté, "Problems of the stub anode connection", Light Metals, (2007), pp. 865-873

[2] K. Grjotheim & H. Kvanda ," Introduction to aluminium electrolysis ", Aluminium-Verlag GmbH ,Dusseldorf (1993)

[3] A. Burkin, "Production of aluminium and alumina", John Wiley & Sons: New York (1987).

[4] K. Grjotheim& B.J.Welch, "Aluminium smelter technology", Aluminium-Verlag GmbH, Dusseldorf (1980).

[5] M. Meier, ″International course on process metallurgy of aluminium″ Trondheim, Norway, (May 2004), p.225.

[6] B. Wood , Aluminium 5, (2007) , pp. 71-73.

[7] A. Sinha," Ferrous physical metallurgy", Butterworth, Boston, (1989).

[8] E. Rollason, "Metallurgy for engineers", Arnold, (1973).

[9] G. Gilbert, "Engineering data on nodular cast irons", British cast iron research association, (1968).

[10] H. Angus, "Physical and engineering properties of cast iron", British cast iron research association, (1960).

[11] M. Barstow, I. Riposan and M. Chismaeria, "Efficient cast iron microstructure for anode –collars in gray or ductile irons", Light Metals, (1997), pp. 619-623.

[12] D. Brooks & V. Bullough, "Factors in the design of reduction cell anodes" Light Metals, (1984), pp. 961- 977.

[13] W. Choate and J. Green, U.S. energy requirements for aluminium production: historical perspective, theoretical limits and new opportunities, (2003).

[14] B. Oye, M.I. Onsoien, E. Haugland, J. Hop, and A. Nordmark," Optimization of the anode-stub contact: material properties of cast iron" Light Metals, (2010) , pp. 1073-1078.

[15] M. M. Ali, A. Nofal, A. Kandil, and M. Agour, "Using of high phosphorus gray iron for the stub- anode connection in the aluminium reduction cells" Journal of Engineering Sciences, Assiut University, Nov.(2011), pp. 1475-1486.

[16] M. Agour, "Cast iron anode fixation collars", M.Sc. thesis, Faculty of Engineering, Al-Azhar University, Cairo, (2011).

[17] A. Nofal, M. Waly, Sh. Mohamed, M. Agour; New solutions for stub-anode connection at Egyptalum, Light Metals (2009) , pp. 1073-1078.

[18] A. Nofal, M. Waly, M. Mourad, A. Kandil , A. Ahmed and M. Agour;" Voltage drop at the stub-anode connection as related carbon equivalent of the cast iron collar", Light Metals,(2010), pp. 961- 977.

[19] J. Davis, "ASM Specialty Handbook - Cast irons", Davis and associates, AMS (1996).

[20] C. Labrecque, M. Martin, D. Lavoie, A. Levesque & M. Murphy "A new technology for cathode rodding used in aluminum electrolytic cells",Light Metals (2003) , pp. 661-667.

[21] ASM Handbook, "Volume 1, Properties and selection: irons, steels, and high-performance alloys", the 4th edition (1995).